Z. Phys. Chem. **227** (2013) 857–868 / **DOI** 10.1524/zpch.2013.0390

Acridine – a Promising Fluorescence Probe of Non-Covalent Molecular Interactions

By Yulia Rozhkova[1], Andrey A. Gurinov[1], Peter M. Tolstoy[1], Gleb S. Denisov[1], Ilya G. Shenderovich[2], and Valentin I. Korotkov[1,*]

[1] St. Petersburg State University, 7-9, Universitetskaya nab., St. Petersburg, 199034 Russia
[2] University of Regensburg, Regensburg, Germany

Dedicated to Prof. Dr. Hans-Heinrich Limbach on the occasion of his 70th birthday

(Received January 21, 2013; accepted in revised form April 1, 2013)
(Published online May 13, 2013)

Hydrogen Bond / Acridine / Acid-Base Complexes / Fluorescence / Proton Transfer

Fluorescence and absorption spectral parameters of acridine have been studied in solution at room temperature in the presence of different proton donors aiming to inspect whether or not acridine can be used as a spectroscopic probe suitable to measure the geometry of hydrogen bonds under different conditions. It has been shown that the most appropriate spectral parameter is the position of fluorescence maximum that changes heavily upon a contraction of the N···H distance. Presumably, also the intensity of the maximum strongly depends on the hydrogen bond geometry. These two parameters can be used to establish two independent, mutually complementary correlations connecting the spectral manifestations and the geometry of hydrogen bond.

1. Introduction

The use of molecular spectroscopic probes is a common strategy in the experimental study of non-covalent molecular interactions. The spectral properties of a molecule selected as a probe should satisfy the following requirements: i) monotonous dependence of the essential spectral parameter on the energy or geometry of the studied interaction; ii) large dynamic range of the spectral changes; iii) detection at low concentration; and iv) adaptability to different states of matter. The requirements are listed in order of their importance. Because of especial chemical and biological importance of hydrogen bonding this ubiquitous interaction was and remains an important target for such studies. For example, the frequency and intensity of the OH stretching vibration have been correlated with the H . . . O distance in OHX hydrogen bonds and their energies [1–7]. However, the application of these correlations for strong hydrogen bonds is often restricted because of anharmonic coupling of this vibration to other

* Corresponding author. E-mail: korotkov@mail.spbu.ru

low-frequency modes [8]. Although, one can identify some other spectroscopic changes which are correlated with hydrogen bond geometry, the amplitude of these changes is generally small as compared to the spectral bandwidths [9,10]. In the past some of us, inspired and driven by H.-H. Limbach, have overcome this problem by employing of ^{15}N NMR of pyridine derivatives. This approach is based on the fact that the isotropic ^{15}N NMR chemical shift of these species depends monotonically on the N···H distance and changes by 125 ppm upon protonation [11,12]. This correlation is especially powerful for strong hydrogen bonds and has been extensively used to measure the N···H distances in hydrogen bonded complexes of pyridine and its derivatives in the liquid [13,14] and solid [15] states and at surfaces [16]. It has revealed the effect of the dielectric permittivity of solvent [17] and specific solvation [18,19] on the geometry of hydrogen bond and has provided understanding of the functional impact of hydrogen bonds in complex application-relevant systems such as amorphous porous materials [20,21] and enzymes [22,23]. Later the application of ^{15}N NMR of pyridines has been extended to other non-covalent interactions as well [24].

Despite its many advantages the use of NMR spectroscopy is associated with the need to keep the concentration of the spectroscopic probe high and to suppress intra- and intermolecular proton and hydrogen bond exchange by using low temperature. In contrast, the use of fluorescence and absorption spectroscopy looks very promising under such circumstances mainly because of its very high sensitivity and short characteristic time-scale [25,26]. Hydrogen bond and proton transfer affect the energies of π-orbitals and lone pairs that can be detected experimentally [27–31]. Previous studies of electronic absorption spectra of nitrogen-containing heterocyclic compounds have demonstrated that protonation results in a reduction of the energy of the first excited electronic level and affects the efficiencies of the first and second electronic transitions [32]. These effects are especially pronounced when the nitrogen is conjugated to a large aromatic system, for example, in acridine. Finally, UV-Vis spectroscopy is clearly applicable to different states of matter.

The aim of this work is to explore the perspectives of acridine as a room temperature molecular spectroscopic probe sensitive to hydrogen bonding and proton transfer. The specific objectives are: (i) to identify a spectral parameter exhibiting the maximal amplitude of changes upon the formation of hydrogen bond and (ii) to inspect whether or not this parameter changes monotonously with the geometry of the hydrogen bond. Special attention has been paid to the position of the maximum of acridine fluorescence. In order to inspect the applicability of this approach to a broad range of hydrogen bond geometries both weak and strong proton donors have been used, namely, alcohols and carboxylic acids. The relative concentrations of the proton donors have been at least two orders of magnitude higher than that of acridine. This condition favors the presence of hydrogen-bonded complexes in solution in sufficient concentration.

2. Experimental section

A fluorescence spectrometer LS 50B and a spectrofluorometer Cary Eclipse have been used to measure the fluorescence of acridine in solution at room temperature. Absorption spectra were obtained on a UV-VIS Spectrophotometer Cary 50 bio.

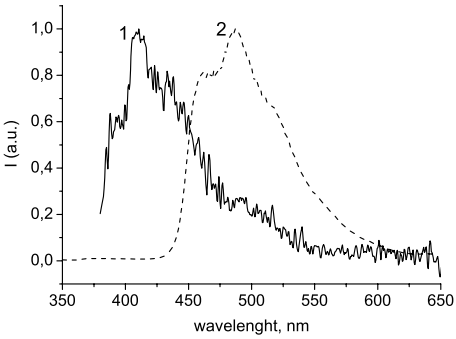

Fig. 1. Normalized fluorescence spectra of: (1) acridine ($C = 6 \times 10^{-5}$ mol/l) and (2) [acridine-H]$^+$BArF$^-$ in CH_2Cl_2, $\lambda_{ex} = 360$ nm.

Solvents purities were: dichloromethane (99.5%) and ethanol (95%). All reagents were purchased from Aldrich with purity of at least 99%. Acridine has been additionally purified by the sublimation. The concentrations of acridine, acids and alcohols were varied in every specific case. A complex of [acridine-H]$^+$ with tetrakis[3,5-bis(trifluoromethyl)phenyl]-borate (BArF$^-$) was obtained as follows: equimolar amounts of acridine and sodium tetrakis[3,5-bis(trifluoromethyl)phenyl]-borate were stirred in 10 ml of water with few drops of hydrochloric acid (37%) for 12 h at 330 K. The precipitated [acridine-H]$^+$BArF$^-$ salt was filtrated, washed with water und dried under vacuum.

3. Results

3.1 Spectral changes upon protonation

In Fig. 1 are depicted the normalized fluorescence spectra of acridine and [acridine-H]$^+$ BArF$^-$ in dichloromethane at room temperature at the excitation wavelength $\lambda_{ex} = 360$ nm. The fluorescence maximum of acridine is located at 411 nm. Protonation of acridine results in a shift of the fluorescence maximum to longer wavelengths up to 487 nm and in increasing of the spectrum intensity. The excitation spectra are given in Fig. 2. The excitation spectrum of [acridine-H]$^+$ BArF$^-$ shows a new band at 380–450 nm, similar to the absorption band, which was studied previously [32].

3.2 Spectral changes upon hydrogen bonding with acids

Interaction of acridine with carboxylic acids of different proton-donating ability has been studied in aprotic dichloromethane at room temperature. Trifluoroacetic acid (TFA, p$K_a = 0.05$), dichloroacetic acid (diClAA, p$K_a = 1.37$), chloroacetic acid (ClAA, p$K_a = 2.65$) and acetic acid (AA, p$K_a = 4.80$) have been used as the proton donors. The pK_a values are given according to [33]. We are aware that the pK_a nomenclature is valid exclusively for aqueous solutions. Thus, these values are reported here only as a qualitative estimation of the expected proton-donating ability.

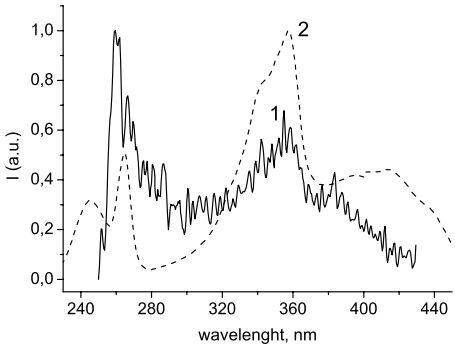

Fig. 2. Normalized excitation spectra in CH_2Cl_2 of: (1) acridine (6×10^{-5} mol/l), $\lambda_{em} = 450$ nm and (2) [acridine-H]$^+$BArF$^-$, $\lambda_{em} = 485$ nm.

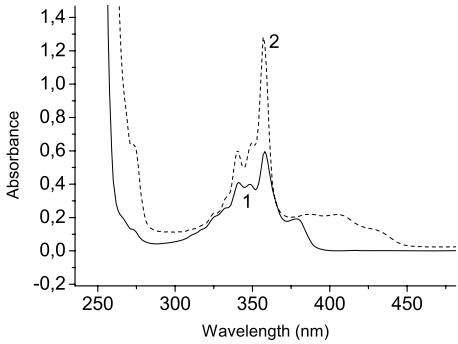

Fig. 3. Absorption spectra in CH_2Cl_2 of: (1) acridine (2×10^{-5} mol/l) and (2) a mixture of acridine (6×10^{-5} mol/l) with TFA (3×10^{-3} mol/l).

The absorption spectra of acridine in the presence of excess of acid are depicted in Fig. 3 (TFA) and 4 (ClAA, AA). The main manifestation of intermolecular hydrogen bond interaction in the case of TFA is the appearance of the new band in the long wavelength region (380–450 nm). For weaker proton donors – ClAA and AA – one can see a spectral broadening of the absorption towards long wavelengths. The spectral changes in fluorescence spectra are pronounced much stronger. Hydrogen bonding to TFA results in a large red shift of the maximum, Fig. 5. The numerical values of the position of the maximum of acridine fluorescence in aprotic solution in dichloromethane in the presence of different acids are listed in Table 1.

For AA the effect of the acid concentration on the fluorescence parameters has been inspected (Fig. 6). When the concentration of AA is low, 2×10^{-3} mol/l, the fluorescence spectrum resembles the one in the absence of acid. An increase of the concentration above 10^{-2} mol/l is accompanied by a discontinuous change of the spectrum and its maximum is shifted close to the value observed in the presence of TFA. For these spectra we have observed a strong increase of the intensity of acridine fluorescence upon the increase of the concentration of AA.

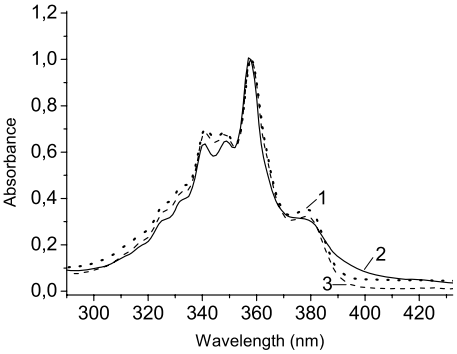

Fig. 4. Absorption spectra in CH_2Cl_2 of: (1) acridine (6×10^{-5} mol/l) and mixtures of acridine (6×10^{-5} mol/l) with (2) ClAA (2×10^{-3} mol/l) and (3) AA (2×10^{-3} mol/l).

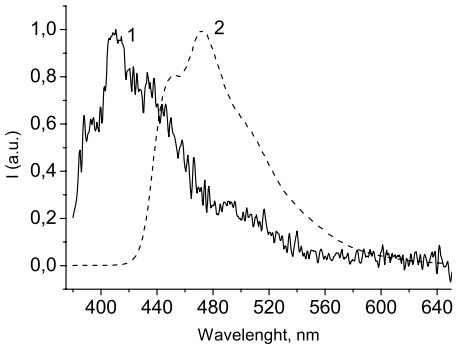

Fig. 5. Normalized fluorescence spectra at $\lambda_{ex} = 360$ nm in CH_2Cl_2 of: (1) acridine (2×10^{-5} mol/l) and (2) a mixture of acridine (6×10^{-5} mol/l) with TFA (10^{-3} mol/l).

Table 1. The position of the fluorescence maximum of acridine in aprotic solution in CH_2Cl_2 in the presence of different carboxylic acids and in different alcohols. The pK_a values of the proton donors are given according to [33]. The concentrations of acridine and carboxylic acids were 10^{-5} and 10^{-3} mol/l, respectively.

Complex	Proton donor pK_a	Fluorescence maximum (nm)
[acridine-H]$^+$BArF$^-$ in CH_2Cl_2	–	487
Acridine + TFA in CH_2Cl_2	0.05	472
Acridine + diClAA in CH_2Cl_2	1.37	469
Acridine + ClAA in CH_2Cl_2	2.65	473
Acridine + AA in CH_2Cl_2	4.80	468
Acridine + PFTB in CH_2Cl_2	7.05	461
Acridine + HFP in CH_2Cl_2	9.75	423
Acridine in ethanol	15.24	413
Acridine in CH_2Cl_2	–	411

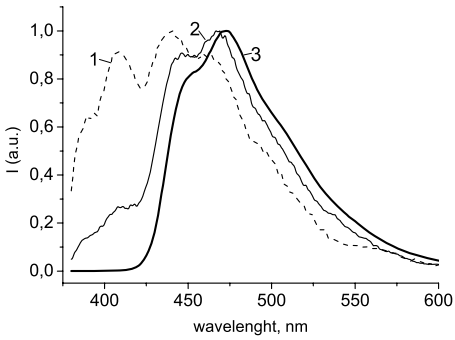

Fig. 6. Normalized fluorescence spectra at λ_{ex} =360 nm in CH_2Cl_2 of mixtures of: (1) acridine (2×10^{-5} mol/l) with AA (2×10^{-3} mol/l), (2) acridine (6×10^{-5} mol/l) with AA (2×10^{-2} mol/l), and (3) acridine (2×10^{-5} mol/l) with AA (1×10^{-2} mol/l).

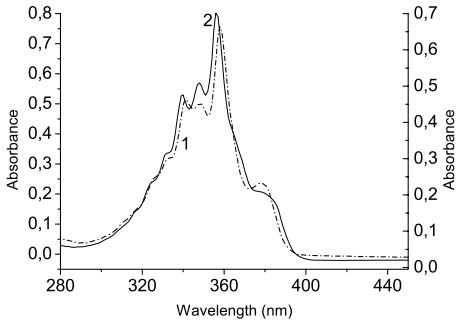

Fig. 7. Absorption spectra of acridine (6×10^{-5} mol/l) in (1) CH_2Cl_2 and (2) ethanol.

3.3 Spectral changes upon hydrogen bonding with alcohols

Interaction of acridine with alcohols has been studied using perfluoro-*tert*-butanol (1,1,1,3,3,3-Hexafluoro-2-(trifluoromethyl)-2-propanol) (PFTB, $pK_a = 7.05$), hexafluoropropanol (HFP, $pK_a = 9.75$), and ethanol ($pK_a = 15.24$). The pK_a values are given according to [33]. In the two former cases acridine and an alcohol have been dissolved in dichloromethane. In the latter case acridine has been dissolved in ethanol. The general trends of the observed spectral changes are the same as in the case of hydrogen bonding with acids. Typical absorption and fluorescence spectra are depicted in Figs. 7 and 8, respectively. The absorption spectrum of acridine practically doesn't change. In contrast, the intermolecular interactions of acridine can be tracked using the position of its fluorescence maximum. The numerical values of the position of the maximum are listed in Table 1. The range of the changes is roughly two-fold larger than for the studied series of carboxylic acids.

The feasibility to use the fluorescence of acridine to discriminate between interactions with different proton donors present in solution has been studied using mixtures of acridine and PFTB dissolved in ethanol. The addition of PFTB results in a broaden-

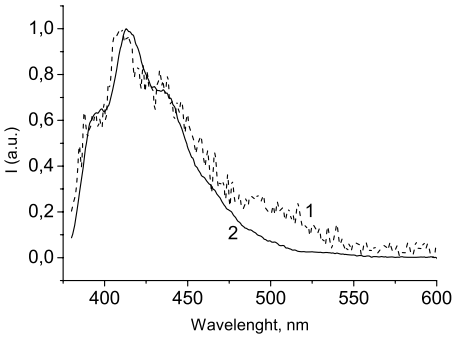

Fig. 8. Normalized fluorescence spectra of acridine (6×10^{-5} mol/l) at $\lambda_{ex} = 360$ nm in (1) CH_2Cl_2 and (2) ethanol.

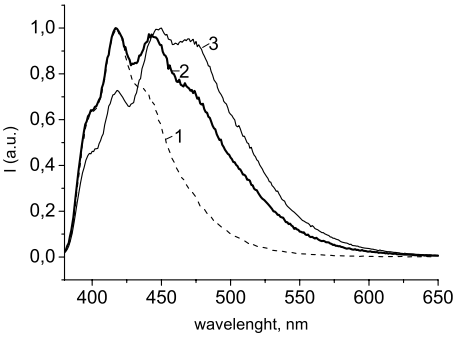

Fig. 9. Normalized fluorescence spectra at $\lambda_{ex} = 355$ nm of acridine (6×10^{-5} mol/l) in ethanol without (1) and in the presence of PFTB: (2) 0.05 mol/l, (3) 0.10 mol/l.

ing of the fluorescence spectra. An increase of its concentration causes a gradual shift of the maximum towards longer wavelengths, Fig. 9. Thus, when the concentration of PFTB is above 0.1 mol/l the spectrum resembles the one of the mixture of acridine and PFTB in dichloromethane.

4. Discussion

In order to solve the aim of this work that is to explore the perspectives of acridine as a molecular spectroscopic probe sensitive to hydrogen bonding and proton transfer, we have studied absorption and fluorescence of acridine in solution in the presence of a number of carboxylic acids and alcohols. The main result obtained in these experiments can be summarized as follows. Fluorescence and absorption spectra of acridine depend on hydrogen bonding and proton transfer. But emission spectra are more sensitive to intermolecular interactions than absorption spectra – the intensity and the position of the fluorescence maximum can be recommended as the spectral parameters of hydrogen bond formation. The fluorescence indicators demonstrate a measureable

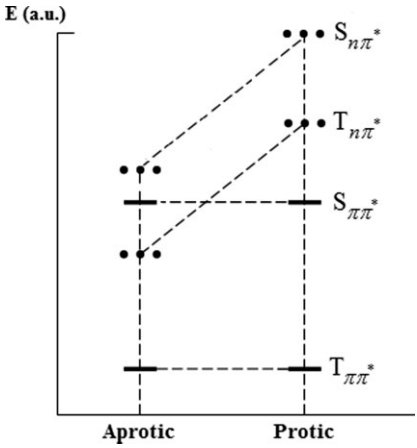

Scheme 1. Inversion of the electronic levels of acridine in protic and aprotic solvents.

change upon an increase of the concentration of AA, while for alcohols this effect is either small or absent. The variation of the relative concentrations of alcohols in their binary mixtures results in a continuous change of the fluorescence parameters that can be attributed to the overlapping of the fluorescence spectra of different acridine-alcohol hydrogen bonded complexes.

Thus, our first specific objective, that was to identify a spectral parameter exhibiting the maximal range of changes upon the formation of hydrogen bonds, has been achieved. This parameter is the position of the fluorescence maximum. The strongest effect has been observed for the [acridine-H]$^+$BArF$^-$ complex that exhibits a 76 nm red shift. In the weakly interacting bulky BArF$^-$ anion the electrical charge is delocalized and cannot affect the geometry of hydrogen bond in the conjugated cation [34,35]. Consequently, the mobile proton is completely transferred to acridine and the N$\cdots$H distance is the shortest possible.

Presumably, also the intensity of the fluorescence maximum can be used as the second, complementary spectral parameter. The activation of the fluorescence of heterocyclic compounds in polar solution is well known [36–40]. It has been observed that an increase of the intensity of fluorescence is usually accompanied by a decrease of the intensity of phosphorescence [37]. This observation led some authors to conclude that hydrogen bonding causes a significant change in the intersystem crossing rate. Consequently, hydrogen bonding may result in the inversion of the $S_{\pi\pi*}$ and the $S_{n\pi*}$ and of the $S_{\pi\pi*}$ and the $T_{n\pi*}$ states of acridine. In the latter case the $S_{\pi\pi*}$ state becomes the lowest one (Scheme 1) [39]. According to estimations within the limits of the Born-Oppenheimer approximation the probability that the intersystem crossing from the lowest $\pi\pi*$ singlet state to an $n\pi*$ triplet state followed by an internal conversion to a phosphorescent triplet state $T_{\pi\pi*}$ is three orders of magnitude higher as compared to the case when the $n\pi*$ singlet state is the lowest one [41]. Thus, the interchange of $S_{\pi\pi*}$ and $T_{n\pi*}$ states due to hydrogen bonding results in an increase of the quantum yield of fluorescence and a decrease of the quantum yield of phosphorescence.

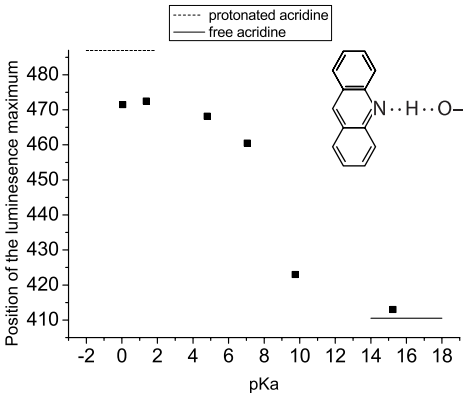

Fig. 10. The dependence of the position of the fluorescence maximum of hydrogen bonded complexes of acridine with various proton donors in dichloromethane *vs.* the pK_a value of the proton donors.

However, the evaluation of the intensity of the fluorescence maximum requires an accurate numerical analysis that is out of the scope of the present work.

Our second specific objective was to inspect whether or not the selected parameter changes monotonously with the geometry of the hydrogen bond. In Table 1 the positions of fluorescence maxima of acridine measured at low concentrations of proton donors in solution in dichloromethane and acridine dissolved in ethanol are listed. The obtained values are correlated with the corresponding pK_a values of the proton-donors in Fig. 10. The proton donating ability of the acids and alcohols has been selectively varied to cover a wide range of hydrogen bond geometries. The sigmoidal correlation curve exhibits limits at 411 nm and 487 nm, which correspond to acridine and the [acridine-H]$^+$ cation, respectively. A similar dependence has been obtained by some of us in the past for a series of proton acceptors interacting with a fixed proton donor [42]. Upon the increase of the proton-donating ability of the donor the mobile proton is gradually shifted towards the acceptor. This process has been studied in detail recently by ^{15}N NMR of pyridine derivatives [11,13]. The position of fluorescence maximum changes slowly when the pK_a of the proton donors is either smaller than 9.75 or large that 7.05. This behavior can be understood taking into account the effect of the electronic excitation on the proton-accepting ability [43]. In the first singlet excited state the pK_a of [acridine-H]$^+$ is about 10.60, while in the ground state it is only 5.50 [44]. We are aware that proton transfer for an acid to a base in a medium with a low dielectric permittivity occurs when the pK_a of the acid is about three units larger than the pK_a of [base-H]$^+$ [11]. Consequently, the electronic excitation of acridine involved in the hydrogen bond in solution in dichloromethane results in the protonation of acridine if the proton donor exhibits in aqueous solution a pK_a larger than 8 or 8.5. The curve in Fig. 10 agrees with this conclusion. The rate constant of the proton transfer is of the order of 10^{-9}–10^{-6} l/mol·s [45]. Thus, the position of fluorescence maximum of acridine depends monotonously on the N···H distance and exhibits a jump upon protonation.

However, varying the concentration of AA we have observed that the position of the fluorescence maximum depends on this concentration, Fig. 6. We attribute these changes to the structure of the hydrogen bonded complexes that are predominant at different concentrations. In a mixture of a nitrogen-containing heterocyclic base and a carboxylic acid there can be 1 : 1 and 2 : 1 acid-base adducts [46,47]. When the acid is in excess but its concentration is low, the 1 : 1 adduct dominates. At high concentrations carboxylic acids dimerize and interact with a base as a pair. The resulting complex contains two hydrogen bonds which can affect each other. This phenomenon is known as a cooperative interaction of conjugated hydrogen bonds [48–50]. Because of this interaction the effective acidity of the non-bonded OH-group of the acid open dimer increases and the proton can be transferred further to the base. What remains unknown is whether the weak changes of the fluorescence parameters at high concentrations of AA are caused by a shift of the equilibrium between 1 : 1 and 2 : 1 or between 2 : 1 and n : 1 ($n > 2$) acid-base structures. Although we expect that this question can be answered using the dependence of the fluorescence parameters on the concentration of AA, this requires an accurate study that is out of the scope of the present work. Thus, we emphasize that the numerical values listed in Table 1 can be affected by the presence of acid-base adducts with structures other than 1 : 1.

5. Conclusion

In the present work we have studied absorption and fluorescence of acridine in solution in dichloromethane in the presence of a number of carboxylic acids and alcohols aiming to inspect whether or not fluorescence and absorption spectral parameters are sensitive to hydrogen bonding and whether or not acridine can be used as a spectroscopic probe suitable to measure the geometry of hydrogen bonds and the effective proton-donating ability of proton-donors under different conditions. It has been shown that the effect of hydrogen bonding on the absorption spectra of acridine is measurable but insufficient to follow the structural changes in detail. In contrast, both the intensity and the position of the fluorescence maximum change dramatically upon the contraction of the N$\cdots$H distance. Consequently, these parameters can be used to establish two independent, mutually complementary correlations connecting the spectral manifestations and the geometry of hydrogen bonds. However, both the establishment of correlations and the practical use of them can be complicated by a strong overlapping of the fluorescence bands of different complexes coexisting in the system under study. At the same time, if the spectral parameters of individual complexes are known, the analysis of experimental spectra can provide the instantaneous relative concentration of different hydrogen bonded species and permits to track the structural changes. It worth to mention that fluorescence spectroscopy exhibits very high sensitivity and requires very low concentration of the spectroscopic probe.

Acknowledgement

This work is supported by the German-Russian Interdisciplinary Science Center (G-RISC) funded by the German Federal Foreign Office *via* the German Academic Exchange Service (DAAD), the Russian Foundation of Basic Research (Projects

11-03-00346 and 11-03-00237) and the grant of Saint-Petersburg State University (11.0.60.2010).

References

1. E. Libowitzky, Monatsh. Chem. **130** (1999) 1047.
2. A. Lautié, F. Froment, and A. Novak, Spectrosc. Lett. **9** (1976) 289.
3. A. Novak, Struct. Bond. **18** (1974) 177.
4. A. V. Iogansen, Spectrochim. Acta A **55** (1999) 1585.
5. N. D. Sokolov, M. V. Vener, and V. A. Savel'ev, J. Mol. Struct. **222** (1990) 365.
6. M. V. Vener, A. N. Egorova, A. V. Churakov, and V. G. Tsirelson, J. Comput. Chem. **33** (2012) 2303.
7. A. Filarowski and A. Koll, Vib. Spectrosc. **17** (1998) 123.
8. Y. Marechal and A. Witkowski, J. Chem. Phys. **48** (1968) 3697.
9. S. M. Melikova, K. S. Rutkowski, A. A. Gurinov, G. S. Denisov, M. Rospenk, and I. G. Shenderovich, J. Mol. Struct. **1018** (2012) 39.
10. S. Kong, I. G. Shenderovich, and M. V. Vener, J. Phys. Chem. A **114** (2010) 2393.
11. P. Lorente, I. G. Shenderovich, N. S. Golubev, G. S. Denisov, G. Buntkowsky, and H.-H. Limbach, Magn. Reson. Chem. **39** (2001) S18.
12. D. V. Andreeva, B. Ip, A. A. Gurinov, P. M. Tolstoy, I. G. Shenderovich, and H.-H. Limbach, J. Phys. Chem. A **110** (2006) 10872.
13. N. S. Golubev, I. G. Shenderovich, S. N. Smirnov, G. S. Denisov, and H.-H. Limbach, Chem.-Eur. J. **5** (1999) 492.
14. P. M. Tolstoy, S. N. Smirnov, I. G. Shenderovich, N. S. Golubev, G. S. Denisov, and H.-H. Limbach, J. Mol. Struct. **700** (2004) 19.
15. S. Kong, A. O. Borissova, S. B. Lesnichin, M. Hartl, L. L. Daemen, J. Eckert, M. Yu. Antipin, and I. G. Shenderovich, J. Phys. Chem. A **115** (2011) 8041.
16. I. G. Shenderovich, G. Buntkowsky, A. Schreiber, E. Gedat, S. Sharif, J. Albrecht, N. S. Golubev, G. H. Findenegg, and H.-H. Limbach, J. Phys. Chem. B **107** (2003) 11924.
17. I. G. Shenderovich, A. P. Burtsev, G. S. Denisov, N. S. Golubev, and H.-H. Limbach, Magn. Reson. Chem. **39** (2001) S91.
18. D. Mauder, D. Akcakayiran, S. B. Lesnichin, G. H. Findenegg, and I. G. Shenderovich, J. Phys. Chem. C **113** (2009) 19185.
19. A. A. Gurinov, D. Mauder, D. Akcakayiran, G. H. Findenegg, and I. G. Shenderovich, ChemPhysChem **13** (2012) 2282.
20. B. C. K. Ip, D. V. Andreeva, G. Buntkowsky, D. Akcakayiran, G. H. Findenegg, and I. G. Shenderovich, Micropor. Mesopor. Mat. **134** (2010) 22.
21. D. Akcakayiran, D. Mauder, C. Hess, T. K. Sievers, D. G. Kurth, I. Shenderovich, H.-H. Limbach, and G. H. Findenegg, J. Phys. Chem. B **112** (2008) 14637.
22. H.-H. Limbach, M. Chan-Huot, S. Sharif, P. M. Tolstoy, I. G. Shenderovich, and G. S. Denisov, BBA-Proteins Proteom. **1814** (2011) 1426.
23. S. B. Lesnichin, I. G. Shenderovich, T. Muljati, H.-H. Limbach, and D. Silverman, J. Am. Chem. Soc. **133** (2011) 11331.
24. A. A. Gurinov, Y. A. Rozhkova, A. Zukal, J. Čejka, and I. G. Shenderovich, Langmuir **27** (2011) 12115.
25. P. M. Tolstoy, B. Koeppe, G. S. Denisov, and H.-H. Limbach, Angew. Chem. Int. Edit. **48** (2009) 5745.
26. B. Koeppe, P. M. Tolstoy, and H.-H. Limbach, J. Am. Chem. Soc. **133** (2011) 7897.
27. E. T. Ryan, T. Xiang, K. P. Johnson, and M. A. Fox, J. Phys. Chem. A **101** (1997) 1827.
28. B. K. Paul and N. Guchhait, J. Lumin. **131** (2011) 1918.
29. Y. H. Liu and P. Li, J. Lumin. **131** (2011) 2116.
30. M. F. Anton and W. R. Moomaw, J. Chem. Phys. **66** (1977) 1808.
31. A. Grabowska, K. Kownacki, and L. Kaczmarek, J. Lumin. **60–61** (1994) 886.

32. Yu. A. Rozhkova, A. A. Gurinov, A. O. Orlova, V. G. Maslov, I. G. Shenderovich, and V. I. Korotkov, Opt. Spectrosc.+ **113** (2012) 275.
33. https://scifinder.cas.org/
34. S. B. Lesnichin, P. M. Tolstoy, H.-H. Limbach, and I. G. Shenderovich, Phys. Chem. Chem. Phys. **12** (2010) 10373.
35. M. Pietrzak, J. P. Wehling, S. Kong, P. M. Tolstoy, I. G. Shenderovich, C. López, R. M. Claramunt, J. Elguero, G. S. Denisov, and H. H. Limbach, Chem.-Eur. J. **16** (2010) 1679.
36. G. G. Guilbault, *Fluorescence, Theory, Practice and Instrumentation*, Marcel Dekker, Inc. New York (1967).
37. N. Mataga, B. Chem. Soc. Jpn. **31** (1958) 459.
38. V. L. Ermolaev and I. P. Kotlyar, Opt. Spectrosc.+ **9** (1960) 353.
39. R. N. Nurmukhametov, D. N. Shigorin, Yu. I. Kozlov, and V. A. Pushkov, Opt. Spectrosc.+ **11** (1961) 327.
40. R. N. Nurmukhametov, Usp. Khim.+ **36** (1967) 1629.
41. M. E. El-Sayed, J. Chem. Phys. **38** (1963) 2834.
42. P. M. Tolstoy, J. Guo, B. Koeppe, N. S. Golubev, G. S. Denisov, S. N. Smirnov, and H.-H. Limbach, J. Phys. Chem. A **114** (2010) 10775.
43. B. M. Uzhinov and M. N. Khimich, Russ. Chem. Rev. **80** (2011) 553.
44. R. Constanciel, O. Chalvet, and J.-C. Rayez, Theoret. Chim. Acta (Berlin) **37** (1975) 305.
45. I. Yu. Martynov, A. B. Demyashkevich, B. M. Uzhinov, and M. G. Kuz'min, Russ. Chem. Rev. **46** (1977) 1.
46. N. S. Golubev, S. N. Smirnov, P. Schah-Mohammedi, I. G. Shenderovich, G. S. Denisov, V. A. Gindin, and H.-H. Limbach, Russ. J. Gen. Chem. **67** (1997) 1082.
47. P. M. Tolstoy, S. N. Smirnov, I. G. Shenderovich, N. S. Golubev, G. S. Denisov, and H.-H. Limbach, J. Mol. Struct. **700** (2004) 19.
48. S. Sharif, I. G. Shenderovich, L. González, G. S. Denisov, D. N. Silverman, and H.-H. Limbach, J. Phys. Chem. A **111** (2007) 6084.
49. I. G. Shenderovich, H.-H. Limbach, S. N. Smirnov, P. M. Tolstoy, G. S. Denisov, and N. S. Golubev, Phys. Chem. Chem. Phys. **4** (2002) 5488.
50. C. Detering, P. M. Tolstoy, N. S. Golubev, G. S. Denisov, and H.-H. Limbach, Dokl. Phys. Chem. **379** (2001) 1.